PAPER

Frequency Domain Nulling Filter and Turbo Equalizer in Suppression of Interference for One-Cell Reused Single-Carrier TDMA Systems

Chantima SRITIAPETCH[†a)], ***Nonmember and*** **Seiichi SAMPEI**[†b)], ***Fellow***

SUMMARY This paper proposes a frequency domain nulling filter and Turbo equalizer to suppress interference in the uplink of one-cell reuse single-carrier time division multiple access (TDMA) systems. In the proposed system, the desired signal in a reference cell is interfered by interference signals including adjacent-channel interference (ACI), co-channel interference (CCI), and intersymbol interference (ISI). At the transmitter, after a certain amount of spectrum is nulled considering the expected CCI, the suppressed power due to nulling is reallocated to the remaining spectrum components so as to keep the total transmit power constant. In this process, when mitigation of ACI is necessary, after a certain amount of spectrum at both edges is nulled using an edge-removal filter, the aforementioned process is conducted. At the receiver, frequency domain SC/MMSE Turbo equalizer (FDTE) is employed to suppress ISI due to spectrum nulling process in the transmitter as well as the multipath fading. Computer simulations confirm that the proposed scheme is effective in suppression of CCI, ACI and ISI in one-cell reuse single-carrier TDMA systems.

key words: *interference suppression, nulling filter, frequency domain turbo equalizer, single-carrier transmission*

1. Introduction

For broadband transmission in the next generation wireless access systems, orthogonal frequency division multiple access combined with time division multiple access (OFDMA/TDMA) is capturing many spotlight due to its high immunity to multipath fading as well as its capability of flexible radio resource management in both time and frequency domains [1]. Especially when a subcarrier-level adaptive modulation is applied to OFDMA/TDMA cellular systems, its robustness to co-channel interference (CCI) can be extremely enhanced; thereby flexible radio resource management based on one-cell reuse cell configuration is applicable even in TDMA based systems [2]. However, there is one serious drawback in OFDMA/TDMA schemes, i.e. high peak to average power ratio (PAPR) due to multicarrier transmission, especially in the uplink transmission.

Single-carrier transmission, on the other hand, has been believed to be unsuitable for broadband transmission due to its high computational complexity in compensation for multipath fading having long channel memory, although its PAPR is much lower than that for OFDMA. But, the situation is now changing. Single-carrier transmission is capturing spotlight again due to feasibility of adaptive equalization with less computation complexity like frequency domain equalizer (FDE), even though channel memory length is relatively long [3]–[8].

When such a broadband single-carrier transmission is applied to cellular systems, however, there is still a remaining challenge; enhancement of immunity to CCI coming from adjacent cells when a single-carrier scheme is introduced in TDMA based cellular systems. In the case of OFDMA based wireless access systems, CCI immunity control is relatively simple, just by controlling the number of bits loaded to each subcarrier according to the channel state information (CSI) including CCI conditions fed back from the receiver side, which is called a subcarrier-level adaptive modulation [9]. In the case of single-carrier transmission, on the other hand, because the transmitted bit stream occupies whole the assigned bandwidth any time, the receiver is always suffering from CCI from adjacent cells in the cellular systems. Thus, energy of such CCI accommodated in the allocated bandwidth has to be efficiently suppressed by some means.

One solution to CCI is to introduce lower symbol rate transmission in adaptive modulation systems. Based on this concept, Ref. [10] proposed a single-carrier TDMA scheme combined with adaptive modulation and frequency domain equalizer. In this scheme, half rate and quarter rate modes are introduced for quaternary phase shift keying (QPSK) in addition to the full rate QPSK, 16-ary quadrature amplitude modulation (16QAM) and 64QAM, and simulation results confirmed that one-cell reuse cell configuration is possible by introduction of such symbol rate controllable adaptive modulation schemes. However, there is still one remaining requirement from the viewpoint of system design, i.e. we would like to further reduce selection probability for lower rates to enhance user throughput even though a user is located in the cell edge.

To solve this problem, we have proposed a nulling filter technique [11] combined with a soft canceller followed by minimum mean square error filter (SC/MMSE) Turbo equalizer [12]–[15] in the receiver side, in which a certain amount of spectrum with lower signal to interference plus noise power ratio (SINR) is nulled in the receiver, and ISI caused by the nulling filter as well as by the multipath fading channel is compensated for using a time domain

Manuscript received April 4, 2008.
Manuscript revised November 23, 2008.

[†]The authors are with the Graduate School of Engineering, Osaka University, Suita-shi, 565-0871 Japan.
a) E-mail: chantima@wireless.comm.eng.osaka-u.ac.jp
b) E-mail: sampei@comm.eng.osaka-u.ac.jp

DOI: 10.1587/transcom.E92.B.2085

SC/MMSE Turbo equalizer. Its important point is that, because SC/MMSE Turbo equalizer, which is classified in the non-linear signal processing type, reproduces soft estimates of the desired signal including the nulled spectrum, thereby it can compensate for channel distortion due to nulling process in addition to the multipath fading. Although the results confirm its effectiveness in suppression of CCI in single-carrier based TDMA systems, it would cause received signal power loss due to discard of partial spectrum in the nulling filter. Moreover, when a discrete Fourier transform (DFT) spread orthogonal frequency division multiplexing (OFDM) is employed as a channelization scheme in the uplink to keep spectrum commonality with OFDMA based downlink signal, adjacent channel interference (ACI) immunity should also be taken into account in the system design. Of course, the nulling filter with an SC/MMSE based Turbo equalizer in the receiver could be one of its solutions, because ACI can be regarded as a special case for CCI. However, the received power for ACI coming from the same cell is, generally speaking, much higher than the CCI coming from adjacent cells in the cellular systems, thereby high level ACI might cause desensitization in the receiver [16]. This means that it is preferable to prevent ACI by creating null spectrum at both edges of the desired signal in the transmitter side.

Creation of null spectrum at both edges might not sound like a serious problem. It is true as long as the spectrum gap is inserted between adjacent channels without changing the signal bandwidth for each user. In such a case, however, symmetry of allocated spectrum between the downlink and uplink is not satisfied.

Thus, this paper proposes a spectrum nulling technique *in the transmitter side* while keeping spectrum symmetry between the downlink and uplink channels to enhance CCI and ACI immunity in one-cell reuse TDMA systems in the uplink; In the proposed scheme, after a certain amount of spectrum is nulled considering the expected CCI, the suppressed power due to nulling is reallocated to the remaining spectrum components so as to keep the total transmit power constant. In this process, when mitigation of ACI is necessary, after a certain amount of spectrum at both edges is nulled using an edge-removal filter, the aforementioned process is conducted. In the receiver side, frequency domain SC/MMSE Turbo equalizer (FDTE) is employed to compensate for ISI due to spectrum nulling process in the transmitter as well as the multipath fading. In this stage, frequency domain Turbo equalizer instead of time domain Turbo equalizer is employed in the receiver because its computation complexity is much lower and it gives better performance due to averaging process conducted in the FDTE [17], [18].

With the proposed algorithm, spectrum commonality with OFDMA based downlink signal can be achieved, thereby the spectrum used in this paper is identical to single carrier orthogonal frequency division multiple access (SC-FDMA); a modified form of OFDMA which is currently a strong candidate for uplink transmission in 3GPP long-term evolution (LTE). In SC-FDMA, when the uplink signal is completely synchronized with the downlink signal, ACI in the uplink is not taken into account. The technique proposed in this paper is to attain ACI immunity even if the uplink signal has frequency jitter due to instability of the carrier frequency. Moreover, although the SC-FDMA applies adaptive modulation and coding (AMC) to achieve higher user rate and enhance interference immunity, one disadvantage of the AMC is, when interference level is increasing, the AMC selects lower user rate to enhance interference immunity. The proposed technique, on the other hand, is to enhance interference immunity without reduction of user rate. There is also one more important issue. Of course, the SC-FDMA can allocate less interfered frequency band to each user in a dynamic spectrum allocation process. However, when the user traffic is getting higher, such a dynamic spectrum allocation becomes less effective, and a band with relatively high CCI might be allocated to a user. Even in such a case, the proposed scheme can be employed to enhance user rate due to its high immunity to CCI. Therefore, when the proposed algorithm is applied to the SC-FDMA in 3GPP LTE, more interference immunity can be expected.

The rest of this paper is organized as follows. Section 2 presents a reference system in which one-cell reuse single-carrier TDMA system is described. Section 3 describes the proposed interference suppression scheme. Section 4 shows the simulation results and Sect. 5 concludes this paper.

2. Reference System and Signal Models

2.1 One-Cell Reuse Single-Carrier TDMA Systems

The concept of one-cell reuse single-carrier TDMA systems for the uplink is shown in Fig. 1. As for generation of the single-carrier signal, carrier interferometry (CI) technique [19], [20] is employed to give spectral compatibility between the single-carrier and OFDM signal. In this system, the desired signal in the reference cell could be interfered by ACI, CCI and ISI: The signals from other users in the same cell would cause ACI because adjacent subcarriers are assigned for another user in the same cell, resulting in potential spectrum overlap due to carrier frequency instability of each terminal. Although such spectrum overlap is not so large, ACI power is sometimes much higher than that for the desired signal, which might result in desensitization in the receiver, and cause severe performance degradation.

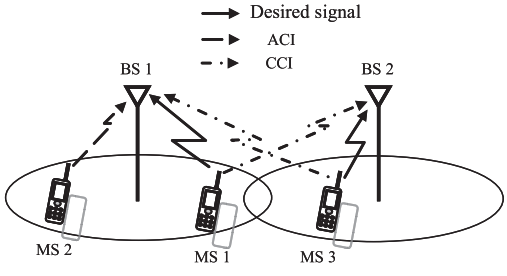

Fig. 1 One-cell reuse cellular system for uplink.

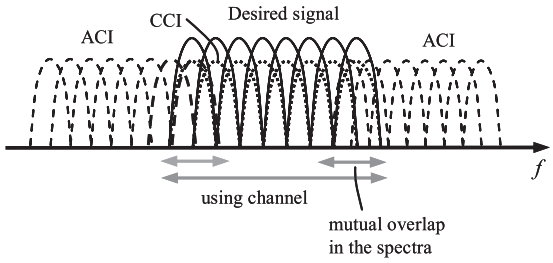

Fig. 2 Spectrum representations of the desired signal with ACI and CCI.

In addition to the ACI, the same frequency reuse in the adjacent cell would cause CCI, and multipath fading would cause ISI. As seen in Fig. 1, at BS1, the desired signal from MS1 is interfered by a signal from MS2 located in the same cell, leading to the ACI. Moreover, the signal from MS3 located in the adjacent cell could cause CCI because the same bandwidth is shared by all the cells in one-cell reuse systems.

Figure 2 shows spectrum representations of the desired signal with ACI and CCI. In this paper, we consider a single-carrier CI/TDMA system for the uplink. CI is a very useful technique to flexibly manipulate spectrum for a single-carrier transmission using almost the same signal processing complexity with OFDM schemes. For example, it can equivalently generate a single-carrier signal with its roll-off factor of zero just by assigning the same amplitude and phase to all the subcarriers of an OFDM symbol. Moreover, at the receiver, the received CI signal has the same features with the OFDM signal.

2.2 Received Signal without Interference Suppression

This section will illustrate the received signal representation of the reference system described above. In this case, interference suppression at the transmitter is not employed and the transmitted signals are the signals after modulation. Let the data signal sequence and interference signal sequence from the outside cell be denoted by $s(t)$; $t = 0, 1, \ldots, K-1$ and $i(t)$; $t = 0, 1, \ldots, K-1$, where K is number of symbols in a block and t is symbol time index. At the receiver, discrete time received signal expressed in the equivalent lowpass system is obtained as

$$r(t) = \underbrace{\sum_{l=0}^{L-1} h_s(l)s(t-l)}_{Desired\ signal} + \underbrace{\sum_{l=0}^{L-1} h_i(l)i(t-l)}_{CCI} + \underbrace{A(t)}_{ACI} + \underbrace{v(t)}_{AWGN} \quad (1)$$

where $h^s(t)$ and $h^i(t)$ are discrete impulse responses for the data signal $s(t)$, and the interference signal $i(t)$, respectively. $v(t)$ is additive white Gaussian noise (AWGN). L denotes channel memory length which is assumed to be identical for both the desired signal and interference signal. It is important to note that the received signal $r(t)$ includes ACI from users in the same cell, denoted by $A(t)$ in (1). Therefore, the received signal $r(t)$ consists of the desired signal, ACI, CCI and AWGN.

3. Proposed System

The configuration of the proposed interference suppression process in the transmitter is shown in Fig. 3, where the figure is expressed in the equivalent lowpass system. After the baseband signal $s(t)$ is transformed into the frequency domain signal format using an FFT, edge-removal filter suppresses potential ACI components by omitting both edges of the spectrum. Then, the nulling filter will suppress spectrum components at which CCI level is expected to be high in the receiver side based on signal to co-channel interference power ratio (SCCIR) information fed back from the receiver. After that, the transmit power allocated to the nulled components is redistributed to the rest of the spectrum to keep the total transmit power constant. The frequency domain signal is then transformed back into time domain signal and the signal is transmitted over the wireless channel. The detailed algorithm including signal representations of each step are explained in the followings:

3.1 Interference Suppression at Transmitter

Step 1) Adjacent Channel Interference Suppression

Frequency domain representation of the data symbol can be obtained by applying K-point FFT operation to $s(t)$, given by

$$S(f) = \sum_{t=0}^{K-1} s(t) \exp\left(-j2\pi \frac{t}{K} f\right) \quad (2)$$

where $f = 0, 1, \ldots, K-1$ denotes frequency component index. When the transmitted data block is expressed in a vector form as $\boldsymbol{s} = [s(0), s(1), \ldots, s(K-1)]^T$, the frequency domain data signal vector can be expressed as

$$\boldsymbol{S} = \boldsymbol{F}\boldsymbol{s} = [S(0), S(1), \ldots, S(K-1)]^T \quad (3)$$

where $\boldsymbol{F}$ is a $K \times K$ DFT matrix defined by

$$\boldsymbol{F} = \frac{1}{\sqrt{K}} \begin{bmatrix} W_K^{0\cdot 0} & W_K^{0\cdot 1} & \cdots & W_K^{0\cdot(K-1)} \\ W_K^{1\cdot 0} & W_K^{1\cdot 1} & \cdots & W_K^{1\cdot(K-1)} \\ \vdots & \vdots & \ddots & \vdots \\ W_K^{(K-1)\cdot 0} & W_K^{(K-1)\cdot 1} & \cdots & W_K^{(K-1)\cdot(K-1)} \end{bmatrix} \quad (4)$$

in which W_K denotes a twiddle factor given by $W_K = \exp(-j2\pi/K)$.

The frequency domain data signal vector $\boldsymbol{S}$ is then fed to the edge-removal filter to prevent potential ACI. Hence, the spectrum after the edge-removal filter can be expressed as

$$\boldsymbol{S}' = \boldsymbol{H}_E\boldsymbol{S} = \begin{bmatrix} H_E(0) & & & \boldsymbol{0} \\ & H_E(1) & & \\ & & \ddots & \\ \boldsymbol{0} & & & H_E(K-1) \end{bmatrix} \begin{bmatrix} S(0) \\ S(1) \\ \vdots \\ S(K-1) \end{bmatrix} \quad (5)$$

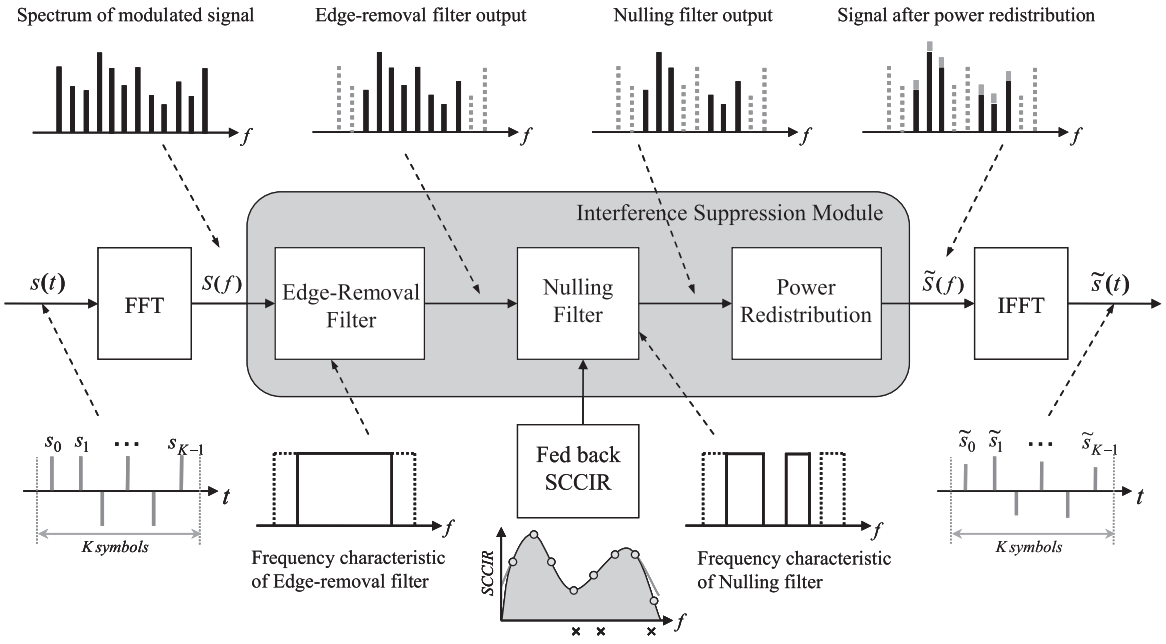

Fig. 3 Interference suppression scheme.

where $\boldsymbol{H}_E = \mathrm{diag}[H_E(0), H_E(1), \ldots, H_E(K-1)]$ denotes a $K \times K$ frequency transfer function matrix of the edge-removal filter, and diagonal elements take zero if the corresponding spectrum is removed, otherwise one.

Step 2) Co-channel Interference Suppression

The frequency domain nulling filter is applied after the edge-removal filter to intentionally suppress the transmitted signal components located in the frequency at which CCI level is expected to be high at the receiver side. The process is the same as the edge-removal filter except that the multiplication by zero is not restricted to the edge spectrum but any spectrum components, and its selection is conducted according to the expected frequency response of the SCCIR fed back from the receiver.

Let us assume that the number of frequency components to be nulled be N_{nu}, frequency components having the lowest N_{nu} SCCIR are nulled, and frequency index of the nulled components be f_i $(i = 1, 2, \ldots, N_{nu})$. The output of the nulling filter can then be expressed as

$$\begin{aligned} \boldsymbol{S''} &= \boldsymbol{H}_{Nu}\boldsymbol{S'} \\ &= \begin{bmatrix} H_{Nu}(0) & & & \boldsymbol{0} \\ & H_{Nu}(1) & & \\ & & \ddots & \\ \boldsymbol{0} & & & H_{Nu}(K-1) \end{bmatrix} \begin{bmatrix} S'(0) \\ S'(1) \\ \vdots \\ S'(K-1) \end{bmatrix} \end{aligned} \tag{6}$$

The spectrum matrix of the nulling filter, denoted by $\boldsymbol{H}_{Nu}$, is the matrix having $H_{Nu}(f)$ in its diagonal components where frequency characteristic of the nulling filter is given by [11]

$$H_{Nu}(f) = \begin{cases} 0, & f = f_i \\ 1, & f \neq f_i \end{cases} \tag{7}$$

Step 3) Power Redistribution

To efficiently utilize the total available transmit power, the transmit power assigned to the nulled spectrum is redistributed to the rest of the spectrum. In this process, when mitigation of ACI is necessary, after a certain amount of edge spectrum is nulled using an edge-removal filter, and a certain amount of spectrum components having lower expected SCCIR is nulled, the transmit power redistribution to the rest of spectrum is conducted considering the amount of nulled spectrum by the edge-removal and nulling filters. Let the total number of nulled spectrum components be denoted by N_s which is the summation of the removed edge-spectrum N_{ed} and the nulled spectrum at nulling filter N_{nu}. First, we can calculate the total transmit power of the spectrum before nulling process as

$$P_t = \mathrm{tr}[E\{\boldsymbol{S} \cdot \boldsymbol{S}^H\}] = \sum_{f=0}^{K-1} |S(f)|^2 = K \tag{8}$$

where $\mathrm{tr}[\boldsymbol{x}]$ denotes the summation of the diagonal elements of the matrix $\boldsymbol{x}$, $E\{\cdot\}$ denotes expectation and $\cdot^H$ denotes Hermitian transpose. Note that the last term in (8) can be obtained according to the assumption that symbol power is normalized to one, i.e. $E\{|s(t)|^2\} = 1$. Thus, the total power of the spectrum after edge-removal and nulling process can be obtained as

$$\begin{aligned} P''_t &= \mathrm{tr}[E\{\boldsymbol{S''} \cdot \boldsymbol{S''}^H\}] \\ &= \mathrm{tr}[E\{\boldsymbol{H}_E\boldsymbol{H}_{Nu}\boldsymbol{S} \cdot \boldsymbol{S}^H\boldsymbol{H}_{Nu}^H\boldsymbol{H}_E^H\}] \\ &= \sum_{f=0}^{K-1} |H_E(f)H_{Nu}(f)|^2 = K - N_s \end{aligned} \tag{9}$$

To maintain the total transmit power to P_t, the signal after

power redistribution becomes

$$\tilde{\boldsymbol{S}} = \delta \boldsymbol{S}'' \tag{10}$$

where δ denotes power redistribution factor which is given by

$$\delta = \sqrt{\frac{P_t}{P_t''}} = \sqrt{\frac{K}{K - N_s}} \tag{11}$$

Thus, the output signal of the interference suppression module can be rewritten as

$$\tilde{\boldsymbol{S}} = \delta \boldsymbol{H}_E \boldsymbol{H}_{Nu} \boldsymbol{S} = \boldsymbol{\Omega S} \tag{12}$$

where $\boldsymbol{\Omega}$ denotes a $K \times K$ spectrum nulling matrix which is diagonal and includes the effect of edge-removal filter, nulling filter and power redistribution process. By applying IFFT to the frequency domain signal given by (12), the time domain transmitted signal is given by

$$\tilde{\boldsymbol{s}} = \boldsymbol{F}^H \tilde{\boldsymbol{S}} = \boldsymbol{F}^H \boldsymbol{\Omega S} = \boldsymbol{F}^H \boldsymbol{\Omega F} \boldsymbol{F}^H \boldsymbol{S} = \boldsymbol{\omega s} \tag{13}$$

where $\boldsymbol{F}^H$ is an IDFT matrix and $\boldsymbol{\omega}$ is the time domain representation of the spectrum nulling process.

3.2 Signal Equalization and Detection at the Receiver

Previous section explains the proposed interference suppression conducted at the transmitter. Specifically, ACI is avoided by creating null spectrum at both edges of the desired signal, and spectrum null is also created at which the CCI level at the receiver is expected to be high. The received signal after nulling can then be expressed as

$$\tilde{r}(t) = \underbrace{\sum_{l=0}^{L-1} h_s(l)\tilde{s}(t-l)}_{Desired\ signal} + \underbrace{\sum_{l=0}^{L-1} h_i(l) i(t-l)}_{CCI} + \underbrace{v(t)}_{AWGN} \tag{14}$$

where $\tilde{s}(t)$ represents t-th component of the transmitted signal after the nulling process. It is important to note that although ACI signal could be removed in this process, $\tilde{r}(t)$ would include degradation due to the ISI caused by the edge-removal filter as well as the nulling filter. To compensate for such ISI, a frequency domain SC/MMSE turbo equalizer (FDTE) is applied in the receiver. The significant point is that FDTE can reproduce soft estimates of the desired signal including nulled spectrum, thereby it can compensate for channel distortion due to nulling process in addition to the multipath fading.

In this paper, we will assume that channel variation in each signal block is stationary. Thus, the received signal vector after cyclic prefix removal $\tilde{\boldsymbol{r}} = [\tilde{r}(0), \tilde{r}(1), \ldots, \tilde{r}(K-1)]^T$ can be expressed as

$$\tilde{\boldsymbol{r}} = \boldsymbol{H}_s^c \tilde{\boldsymbol{s}} + \boldsymbol{H}_i^c \boldsymbol{i} + \boldsymbol{v} \tag{15}$$

where $\boldsymbol{H}_s^c$ and $\boldsymbol{H}_i^c$ denote the channel matrices of the transmitted signal and interference signal, respectively. Note that $\boldsymbol{H}_s^c$ and $\boldsymbol{H}_i^c$ are circulant matrices with their first column vectors of $[h_s(0), h_s(1), \ldots, h_s(L-1), \boldsymbol{0}_{K-L}]^T$ and $[h_i(0), h_i(1), \ldots, h_i(L-1), \boldsymbol{0}_{K-L}]^T$, where $\boldsymbol{0}_{K-L}$ denotes consecutive zero vector of length $K-L$. Since frequency domain signal equalization is employed in this system, the received spectrum vector $\tilde{\boldsymbol{R}} = [\tilde{R}(0), \tilde{R}(1), \ldots, \tilde{R}(K-1)]^T$ can be expressed as

$$\begin{aligned}\tilde{\boldsymbol{R}} &= \boldsymbol{F}\tilde{\boldsymbol{r}} = \boldsymbol{F}\boldsymbol{H}_s^c\tilde{\boldsymbol{s}} + \boldsymbol{F}\boldsymbol{H}_i^c\boldsymbol{i} + \boldsymbol{F}\boldsymbol{v} \\ &= \boldsymbol{F}\boldsymbol{H}_s^c\boldsymbol{F}^H\boldsymbol{F}\tilde{\boldsymbol{s}} + \boldsymbol{F}\boldsymbol{H}_i^c\boldsymbol{F}^H\boldsymbol{F}\boldsymbol{i} + \boldsymbol{F}\boldsymbol{v} \\ &= \boldsymbol{\Xi}_s\tilde{\boldsymbol{S}} + \boldsymbol{\Xi}_i\boldsymbol{I} + \boldsymbol{V} = \boldsymbol{\Xi}_s\boldsymbol{\Omega}\boldsymbol{S} + \boldsymbol{\Xi}_i\boldsymbol{I} + \boldsymbol{V} \\ &= \tilde{\boldsymbol{\Xi}}_s\boldsymbol{S} + \boldsymbol{\Xi}_i\boldsymbol{I} + \boldsymbol{V}\end{aligned} \tag{16}$$

where $\boldsymbol{I} = \boldsymbol{F}\boldsymbol{i} = [I(0), I(1), \ldots, I(K-1)]^T$ and $\boldsymbol{V} = \boldsymbol{F}\boldsymbol{v} = [V(0), V(1), \ldots, V(K-1)]^T$ are interference and noise spectrum vectors, respectively. $\boldsymbol{\Xi}_s$ and $\boldsymbol{\Xi}_i$ denote frequency domain channel matrices of $\boldsymbol{H}_s^c$ and $\boldsymbol{H}_i^c$ given by

$$\boldsymbol{\Xi}_s = \boldsymbol{F}\boldsymbol{H}_s^c\boldsymbol{F}^H = \mathrm{diag}[\Xi_s(0), \Xi_s(1), \ldots, \Xi_s(K-1)] \tag{17}$$

and

$$\boldsymbol{\Xi}_i = \boldsymbol{F}\boldsymbol{H}_i^c\boldsymbol{F}^H = \mathrm{diag}[\Xi_i(0), \Xi_i(1), \ldots, \Xi_i(K-1)] \tag{18}$$

Moreover, the product of frequency domain channel matrix $\boldsymbol{\Xi}_s$ and nulling matrix $\boldsymbol{\Omega}$, which is expressed as $\tilde{\boldsymbol{\Xi}}_s$ in (16), represents the equivalent channel matrix that includes both nulling at the transmitter and the channel.

In FDTE, soft estimate which is the expectation of the desired signal vector $\hat{\boldsymbol{s}} = [\hat{s}(0), \hat{s}(1), \ldots, \hat{s}(K-1)]^T$ is calculated using extrinsic log-likelihood ratio (LLR) fed back from the decoder. The residual interference is then generated in the soft interference cancellation process as

$$\hat{\boldsymbol{R}} = \tilde{\boldsymbol{R}} - \tilde{\boldsymbol{\Xi}}_s\hat{\boldsymbol{S}} \tag{19}$$

where $\hat{\boldsymbol{S}} = [\hat{S}(0), \hat{S}(1), \ldots, \hat{S}(K-1)]^T = \boldsymbol{F}\hat{\boldsymbol{s}}$ denotes the soft estimate spectrum vector. From (16), $\hat{\boldsymbol{R}}$ can be rewritten as

$$\begin{aligned}\hat{\boldsymbol{R}} &= (\tilde{\boldsymbol{\Xi}}_s\boldsymbol{S} + \boldsymbol{\Xi}_i\boldsymbol{I} + \boldsymbol{V}) - \tilde{\boldsymbol{\Xi}}_s\hat{\boldsymbol{S}} \\ &= \tilde{\boldsymbol{\Xi}}_s(\boldsymbol{S} - \hat{\boldsymbol{S}}) + \boldsymbol{\Xi}_i\boldsymbol{I} + \boldsymbol{V}\end{aligned} \tag{20}$$

Next, the frequency domain MMSE filter will compensate for the residual interference and ISI iteratively. The output of the equalizer can be calculated as [18]

$$\boldsymbol{z} = (1 + \gamma\delta)^{-1}[\gamma\hat{\boldsymbol{s}} + \boldsymbol{F}^H\boldsymbol{\Xi}_s^H\boldsymbol{\Psi}^{-1}\hat{\boldsymbol{R}}] \tag{21}$$

where

$$\gamma = \frac{1}{K}\mathrm{tr}[\tilde{\boldsymbol{\Xi}}_s^H\boldsymbol{\Psi}^{-1}\tilde{\boldsymbol{\Xi}}_s] \tag{22}$$

$$\boldsymbol{\Psi} = E\{\hat{\boldsymbol{R}}\hat{\boldsymbol{R}}^H\} = \tilde{\boldsymbol{\Xi}}_s\boldsymbol{\Delta}\tilde{\boldsymbol{\Xi}}_s^H + \boldsymbol{\Xi}_i\boldsymbol{\Xi}_i^H + N_0\boldsymbol{I}_K \tag{23}$$

$$\boldsymbol{\Delta} = (1 - \delta)\boldsymbol{I}_K \tag{24}$$

$$\delta = \frac{1}{K}\sum_{k=1}^{K}|\hat{s}(k)|^2 \tag{25}$$

and N_0 is the noise spectral density.

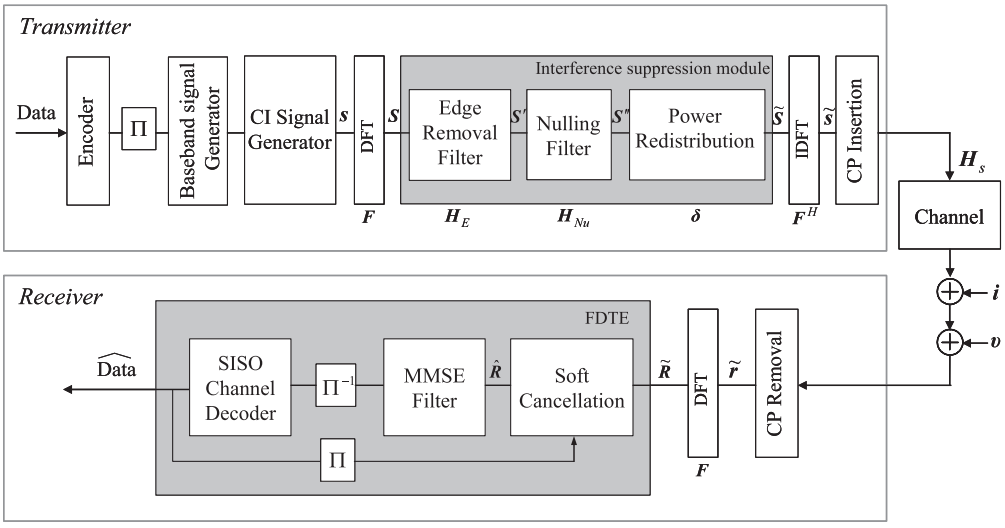

Fig. 4 Transmitter and receiver configuration.

3.3 Configuration of the Proposed System

The transmitter and receiver configuration of the proposed system is depicted in Fig. 4, where this figure is expressed in the equivalent lowpass system. Data bit sequence is first encoded, interleaved and fed to a baseband signal generator to generate a modulated symbol sequence.

After that, CI signal generation process is operated to generate a single-carrier signal [21]. Specifically, when the same amplitude and phase is applied to all the subcarriers, an impulse having a sync waveform can be generated. When a linear phase offset is applied instead of the same phase value, timing of the pulse can be controlled. This means that the CI signal can be regarded as a single-carrier baseband signal filtered by a root Nyquist filter with its roll-off factor of zero. Thus, based on these principles, single-carrier signal vector having spectrum compatible to OFDM, $\boldsymbol{s}$ (block length of K), can be generated. The data signal vector is then converted to frequency domain signal using a DFT matrix. After that, according to the procedure mentioned in the previous section, the DFT output is fed to the edge-removal filter followed by a nulling filter. After the transmit power redistribution to the rest of spectrum is conducted, the output spectrum $\tilde{\boldsymbol{S}}$ is transformed back into the time domain via an IDFT. Cyclic prefix (CP) is then appended at the head of each transmitted signal block.

At the receiver, after the CP is removed to obtain the received signal block $\tilde{\boldsymbol{r}}$, it is converted to the frequency domain signal $\tilde{\boldsymbol{R}}$, which is forwarded to the FDTE. In the FDTE, soft replica of the transmitted signal is generated using the extrinsic log-likelihood ratio (LLR) of the SISO decoder, and it is used to subtract the ISI components from the received signal. A linear filter whose taps are adjusted based on MMSE criterion (MMSE filter) is applied to suppress residual ISI. The extrinsic LLR calculated from the filter outputs is then fed to channel decoder as its *a priori* information. Finally, SISO decoding is performed to extract the estimated data signal.

4. Simulation Results

Computer simulations have been conducted to evaluate the performance enhancement of the proposed algorithm. Table 1 summarizes the simulation parameters. The simulations assume that user located in the reference cell as well as user from adjacent cell experience 24-path Rayleigh fading channel. It is also assumed that channel and SCCIR estimations are perfectly conducted since our group has already developed such techniques [21], [22]. A half-rate non-systematic convolutional code with its constraint length of 3 is used. Each block consists of 256 data symbols. At the receiver, the FDTE is utilized for equalization and Log-MAP algorithm is used in the SISO channel decoder.

The desired signal in the reference cell is assumed to be interfered by an interference signal with a certain signal power ratio where the ratio of desired signal power to CCI signal power is denoted by SCCIR and the ratio of desired signal power to ACI signal power is denoted by SACIR. Under these conditions, system performances are evaluated in the case only CCI is considered and when both CCI and ACI simultaneously occur.

4.1 No ACI Case

Figure 5 shows the block error rate (BLER) performances of the proposed algorithm as a function of transmitted E_s/N_0 when binary phase shift keying (BPSK) is used as a modulation scheme and SCCIR is equal to 5 dB. In this paper, a block means an FFT block. Thus, a block error means that at least one bit is incorrectly detected in an FFT block. The performance without interference suppression is shown in a dot line while the proposed interference suppression algorithm performances are plotted in solid lines. Figure 5 also

Table 1 Simulation parameters.

Block length (K)	256 symbols
Modulation	BPSK, QPSK
Encoder	Convolutional code (R = ½) constraint length = 3
Number of antennas	Tx : 1, Rx : 1
Channel model	24-path Rayleigh Fading
Channel estimation	Perfect
Number of subcarriers (N_f)	256
Removed edge-components (N_{ed})	4, 8, 16, 32, 64
Nulled components (N_{nu})	64, 128
Equalizer	Frequency domain SC/MMSE Turbo Equalizer (FDTE)
Decoder	Log-MAP
Num. of decoding iteration	4

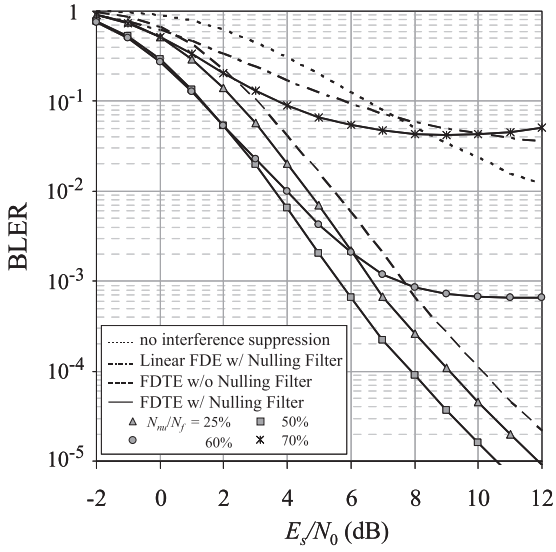

Fig. 5 BLER vs. E_s/N_0 when SCCIR = 5 dB.

includes the performance when FDTE is used at the receiver but no nulling process is conducted at the transmitter which is shown in the figure as a dash line.

It is seen that the proposed algorithm which applies FDTE and nulling process with nulling factor (N_{nu}/N_f) of 50 percent gives the best performance. Specifically, system without any interference suppression suffers from CCI so that it could not achieve BLER under 10^{-2}. Compared to FDTE without nulling filter, the proposed algorithm is approximately 2 dB better for BLER = 10^{-4}.

To evaluate the effect of equalization algorithm in conjunction with the nulling process, FDTE is replaced by a linear frequency domain equalizer (Linear FDE) and the performance is plotted in the figure as a dash-dot line. It is obvious that the FDTE is much more effective than the Linear FDE to compensate for extra ISI produced by the nulling process. In addition, the impact of nulling factor is also investigated and the performances with nulling factor of 25, 50, 60 and 70 percent are plotted in the same figure. It is found that nulling factor of 50 percent is optimum because when nulling factor is increased to 60 and 70 percent, the

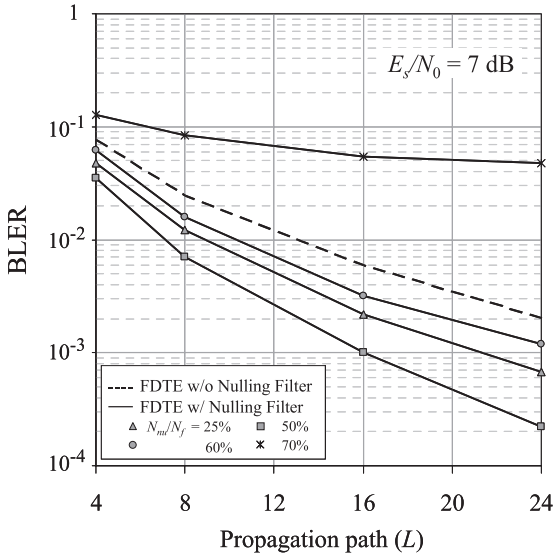

Fig. 6 BLER vs. Propagation path.

FDTE does not converge.

To further examine the relationship between nulling factor and fading channel characteristics, the BLER performances with different numbers of propagation path are plotted and shown in Fig. 6. This graph confirms that nulling factor of 50 percent is optimum regardless of the numbers of propagation path. The reason can be considered as follows: Although extra ISI is induced by the nulling process in the transmitter side, such ISI can be compensated for by the FDTE. One more important issue is that nulling is applied to spectrum components with lower SCCIR and the transmit power is redistributed to the rest of the spectrum so that the total transmit power is kept constant regardless of the nulling factor. Specifically, the energy which should be essentially assigned to the spectrum components with smaller SCCIR is assigned to the spectrum components with higher SCCIR. This means that the received energy is concentrated more on spectrum components with higher SCCIR with increase of the nulling factor in the proposed scheme, and it is more effective when larger nulling factor is employed as long as convergence of the FDTE is guaranteed. Thus, the optimum number of the nulling factor is less sensitive to the number of the path (L), although the BLER performance is improved with the number of L.

Figure 7 shows BLER versus SCCIR when E_s/N_0 are 4 and 10 dB. The performances are compared between the conventional FDTE and the proposed algorithm with nulling factor of 25 and 50 percent. It is seen that the proposed algorithm gives a much higher tolerance to CCI compared to FDTE without nulling filter. At E_s/N_0 = 4 dB, the proposed algorithm can reach BLER of 10^{-2} when SCCIR is approximately 4 dB while the conventional algorithm can achieve the same BLER level when SCCIR increases to 8 dB. Similar results can be observed at E_s/N_0 = 10 dB.

In the actual cell configuration, SCCIR is determined by the statistics of the terminal location. Thus, when the ac-

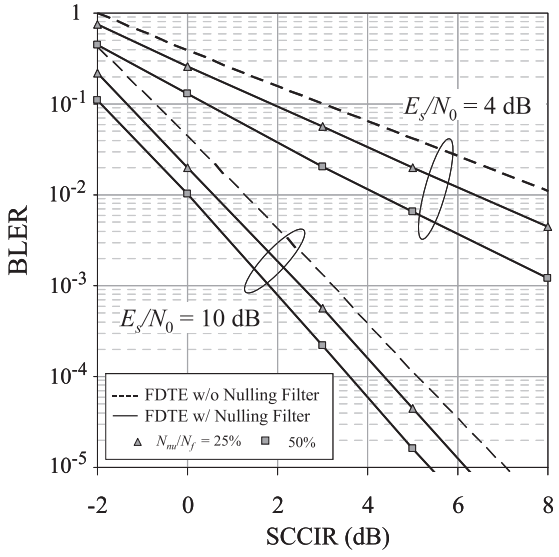

Fig. 7 BLER vs. SCCIR.

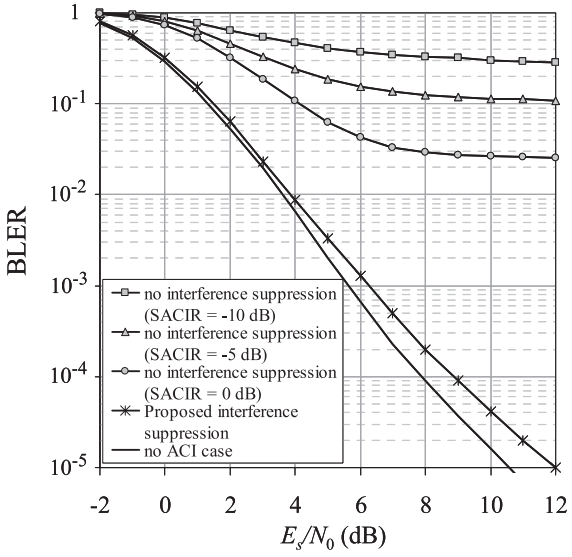

Fig. 9 BLER vs. E_s/N_0 when SCCIR = 5 dB and SACIR = −10, −5, 0 dB.

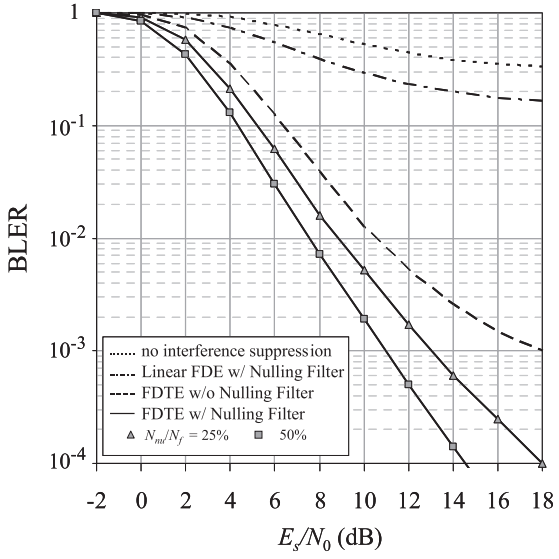

Fig. 8 BLER performance of QPSK modulation.

tual system level evaluation, such as the throughput or message delay performances, is necessary, we have to conduct multi-cell and multi-user simulation. However, our focus point is, as explained in introduction, reduction of selection probability of lower symbol rate transmission in the single-carrier TDMA scheme. In other words, improvement of robustness to CCI without reduction of the symbol rate. Thus, BLER vs. SCCIR performances are evaluated. It is seen in Fig. 7 that the proposed algorithm with nulling factor of 50 percent outperform the proposed algorithm with nulling factor of 25 percent and the conventional FDTE at any value of SCCIR, because the proposed technique concentrates the received energy to spectrum with higher SCCIR, thereby enhance robustness to interference.

Figure 8 shows the BLER performance of the proposed algorithm when QPSK is applied as a modulation scheme. The system without interference suppression and the system applying Linear FDE with nulling filter severely suffer from CCI, while the proposed FDTE with nulling filter still provides good performance. The results confirm that the proposed algorithm is effective in increase of selection probability of full rate QPSK and BPSK, when adaptive modulation and coding is employed in the single-carrier TDMA systems.

4.2 Both CCI and ACI Existence Case

Simulation results when the desired signal experiences both CCI and ACI will be shown in this section. Here, the system employs $N_f = 256$ subcarriers to transmit 256 data symbols. CCI is generated over the entire bandwidth while ACI interferes with the signal by N_{ed} subcarriers. In the proposed system, it is assumed that the carrier frequency f_c is 4 GHz, instability of carrier frequency Δf is $10^{-6} f_c$ which is equal to 4 kHz, and symbol rate is 256 ksps. On this assumption, the number of spectrum interfered at each edge in the worst case becomes $(\frac{4\times10^3}{256\times10^3})N_f$. Since the system employs 256 subcarriers, interference spectrum at each edge is equal to 4 subcarriers or totally 8 subcarriers at both edges, i.e. N_{ed} = 8 subcarriers. When symbol rate is changed to 128 or 512 ksps, N_{ed} is 16 or 4 subcarriers, respectively.

Figure 9 illustrates the BLER versus E_s/N_0 performance of the proposed system in the presence of CCI and ACI. In this simulation, SCCIR is equal to 5 dB and N_{ed} = 8 subcarriers (8 subcarriers are suffering from ACI due to carrier frequency jitter). In Fig. 9, five cases are presented: 1) no ACI is present; 2) the proposed interference suppression algorithm employed case; 3) no interference suppression employed case when SACIR = 0 dB; 4) no interference suppression employed case when SACIR = −5 dB; and 5)

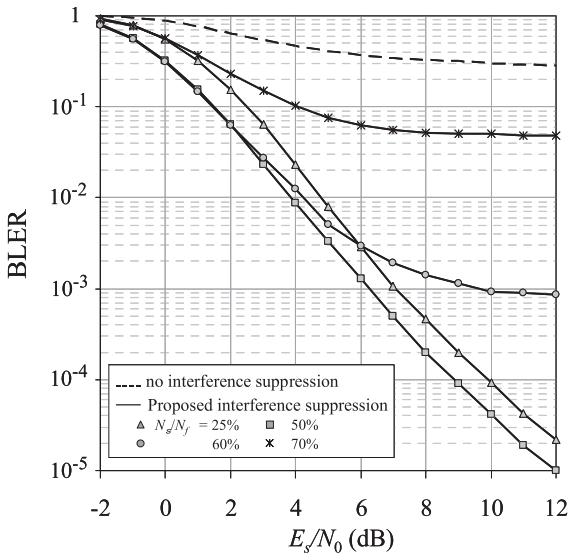

Fig. 10 BLER performance with different numbers of overall nulling factors.

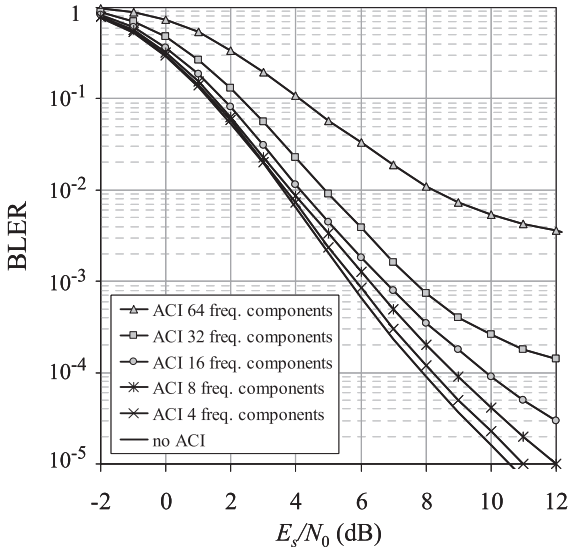

Fig. 11 BLER performance with different numbers of ACI components when SCCIR = 5 dB and SACIR = −10 dB.

no interference suppression employed case when SACIR = −10 dB. In the proposed scheme employed case, because the BLER performances for ACI = −10, −5, and 0 dB cases show completely the same, only one line is shown in this figure. It is seen from the figure that when interference suppression is not employed, the BLER performances are severely degraded and it is getting worse as SACIR becomes low. On the other hand, when the proposed technique is employed, the performance degradation is graceful and no error floor is observed. Moreover, the performances of the proposed scheme are confirmed not to be affected by the SACIR value because edge-removal process in the transmitter prevents spectrum overlapping between the desired and adjacent signals.

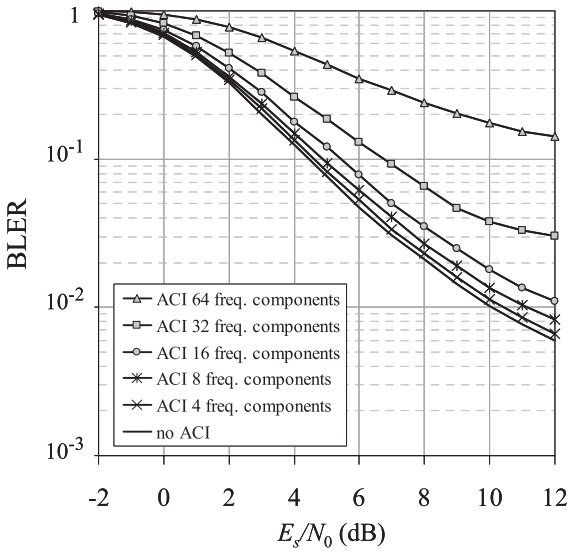

Fig. 12 BLER performance with different numbers of ACI components when SCCIR = 0 dB and SACIR = −10 dB.

The impact of nulling factor when the system experiences both CCI and ACI is also observed as depicted in Fig. 10. The results are similar to the case without ACI which show that overall nulling factor (N_s/N_f) of 50 percent gives the best performance.

Figures 11 and 12 illustrate BLER performances with the number of carriers experiencing ACI as a parameter. Figure 11 shows performance when SCCIR = 5 dB while Fig. 12 shows performance when SCCIR = 0 dB. In both figures, SACIR = −10 dB is assumed. The influence of number of ACI components on the BLER performance can be investigated in these figures. The number of ACI components is varied from 0 (no ACI) to 64 frequency components. It is found that reasonable BLER can be maintained if ACI components are less than 16 components. Generally, the ratio of the guard band to the total bandwidth of a few percent is employed in most systems. Thus, this result shows that the proposed scheme is effective in suppression of ACI due to frequency jitter.

5. Conclusions

This paper has proposed a novel interference suppression algorithm employing frequency domain edge-removal filter and nulling filter combined with frequency domain SC/MMSE turbo equalizer (FDTE). ACI and CCI effects from other users are suppressed by the edge-removal filter and nulling filter operated in frequency domain, respectively. Although these frequency domain filters increase the ISI imposed on the received signals, the FDTE applied at the receiver can compensate for this ISI as well as ISI induced by the fading channel. Computer simulations confirm that the proposed system can effectively suppress CCI. Moreover, it is also effective in suppression of the ACI even if interference signal power is high.

References

[1] H. Harada, C. Ahn, S. Takahashi, Y. Kamio, and S. Sampei, "New generation mobile communication system by dynamic parameter controlled OF/TDMA," IEICE Technical Report, RCS2003-284, Jan. 2004.
[2] T. Nakanishi, S. Sampei, H. Harada, and N. Morinaga, "An OFDM based adaptive modulation scheme employing variable coding rate," IEICE Trans. Commun., vol.E88-B, no.2, pp.526–534, Feb. 2005.
[3] D. Falconer, S.L. Ariyavisitakul, A. Benyamin-Seeyar, and B. Eidso, "Frequency domain equalization for single-carrier broadband wireless systems," IEEE Commun. Mag., vol.40, no.4, pp.58–66, April 2002.
[4] N. Al-Dhahir, "Single-carrier frequency-domain equalization for space-time-coded transmissions over broadband wireless channels," Proc. 12th IEEE International Symposium on Personal, Indoor and Mobile Radio Communications, vol.1, pp.143–146, Sept. 2001.
[5] M.V. Clark, "Adaptive frequency-domain equalization and diversity combining for broadband wireless communications," IEEE J. Sel. Areas Commun., vol.16, no.8, pp.1385–1395, Oct. 1998.
[6] J.P. Coon and M.A. Beach, "An investigation of MIMO single-carrier frequency-domain MMSE equalization," Proc. London Communications Symposium, pp.237–240, 2002.
[7] B. Ng, D. Falconer, K. Kansanen, and N. Veselinovic, "Frequency domain iterative methods for detection and estimation," Proc. 14th IST Mobile & Wireless Communications Summit, in CD ROM, June 2005.
[8] R. Dinis, D. Falconer, and B. Ng, "Iterative frequency-domain equalizers for adjacent channel interference suppression," Proc. IEEE Globecom. 2005, vol.6, pp.3581–3585, Nov. 2005.
[9] S. Sampei and H. Harada, "System design issues and performance evaluations for adaptive modulation in new wireless access systems," Proc. IEEE, vol.95, no.12, pp.2456–2471, Dec. 2007.
[10] K. Kadooka and S. Sampei, "A study on inter-cell interference suppression using frequency domain equalizer for one-cell reuse broadband TDMA systems," IEICE Technical Report, RCS2004-265, Jan. 2005.
[11] C. Sritiapetch and S. Sampei, "Co-channel interference suppression scheme employing nulling filter and Turbo equalizer for single-carrier TDMA systems," IEICE Trans. Commun., vol.E90-B, no.7, pp.1857–1860, July 2007.
[12] X. Wang and H.V. Poor, "Iterative (Turbo) soft interference cancellation and decoding for coded CDMA," IEEE Trans. Commun., vol.47, no.7, pp.1046–1061, July 1999.
[13] D. Reynolds and X. Wang, "Low-complexity turbo-equalization for diversity channels," Signal Process., vol.81, no.5, pp.989–995, May 2000.
[14] T. Abe and T. Matsumoto, "Space-time turbo equalization in frequency selective MIMO channels," IEEE Trans. Veh. Technol., vol.52, no.3, pp.469–475, May 2003.
[15] T. Abe, S. Tomisato, and T. Matsumoto, "A MIMO turbo equalizer for frequency-selective channels with unknown interference," IEEE Trans. Veh. Technol., vol.52, no.3, pp.476–482, May 2003.
[16] J.J. Gavan and M.B. Shulman, "Effects of desensitization on mobile radio system performance, Part I: Qualitative analysis," IEEE Trans. Veh. Technol., vol.VT-33, no.4, pp.285–290, Nov. 1984.
[17] M. Tücher and J. Hagenauer, "Turbo equalization using frequency domain equalizers," Proc. Allerton Conference, pp.1234–1243, Oct. 2000.
[18] K. Kansanen, Wireless broadband single-carrier systems with MMSE Turbo equalization receiver, Ph.D. Dissertation, University of Oulu, Finland, Dec. 2005, (http://herkules.oulu.fi/isbn9514279336/isbn9514279336.pdf)
[19] B. Natarajan, C.R. Nassar, and S. Shatti, "Throughput enhancement in TDMA through carrier interferometry pulse shaping," Proc. IEEE VTC2000-Fall, vol.4, pp.1799–1803, Sept. 2000.
[20] B. Natarajan, C.R. Nassar, and S. Shatti, "Innovative pulse shaping for high-performance wireless TDMA," IEEE Commun. Lett., vol.5, no.9, pp.372–374, Sept. 2001.
[21] K. Yokomakura, S. Sampei, H. Harada, and N. Morinaga, "A carrier interferometry based channel estimation technique for one-cell reuse MIMO-OFDM/TDMA cellular systems," Proc. IEEE VTC2006-Spring, vol.4, pp.1733–1737, May 2006.
[22] T. Ohnishi and S. Sampei, "A study on received SINR estimation technique for OFDM adaptive modulation-based one-cell reuse TDMA systems," IEICE Technical Report, RCS2006-6, April 2006.

Chantima Sritiapetch received the B.E. degree in electrical engineering from Kasetsart University, Bangkok, Thailand in 2000 and the M.E. degree in electrical engineering from Chulalongkorn University, Bangkok, Thailand in 2003. She received the Monbukagakusho Scholarship from Japanese Government in 2003 and became a research student at the Department of Information and Communications Technology, Graduate School of Engineering, Osaka University, Japan where she is currently working toward the Ph.D. Her research interests include Turbo equalizer, interference suppression and digital signal processing for wireless communications.

Seiichi Sampei received the B.E., M.E. and Ph.D. degrees in electrical engineering from Tokyo Institute of Technology, Japan, in 1980, 1982 and 1991, respectively. From 1982 to 1993, he was engaged in the development of adjacent channel interference rejection, fast fading compensation and M-ary QAM techniques for land-mobile communication systems, as a researcher in the Communications Research Laboratory, Ministry of Posts and Telecommunications, Japan. During 1991 to 1992, he was at the University of California, Davis, as a visiting researcher. In 1993, he joined the Faculty of Engineering, Osaka University, and he is currently a Professor in the department of Information and Communications Technology, Osaka University, where he has developed adaptive modulation, intelligent radio transmission/access, and cognitive wireless networking techniques. He received the Shinohara Young Engineering Award, the Achievements Award from the IEICE (Institute of Information and Communication Engineers), the Telecom System Technology Award from the Telecommunication Advancement Foundation, and the DoCoMo Mobile Science Award from Mobile Communication Fund. He is a member of the Institute of Image Information and Television Engineers (ITE) and a Fellow of the IEEE.